for $m, n = 1, 2, 3, \ldots, N$. An additional matrix $[B]$ is defined with elements b_{mn} given, for the same range of m and n, by

$$b_{mn} = \begin{cases} \text{sinc } [(n-m)kd] + \text{sinc } [(n+m-1)kd] & \text{symmetric} \\ \text{sinc } [(n-m)kd] - \text{sinc } [(n+m-1)kd] & \text{antisymmetric} \end{cases}$$

Then the directivity in direction θ is given as the ratio of quadratic forms,

$$D(\theta) = \frac{2[J]^t[A][J]}{[J]^t[B][J]}$$

Finally, the discrete array equivalent of the normalised boresight difference slope, defined by Kirkpatrick[5] for a continuous line source, is found to be[4]

$$K = \frac{[K]^t[J]}{\sqrt{(2[J]^t[B_d][J])}}$$

where

$$[K] = \frac{1}{2N-1}\begin{bmatrix} 1 \\ 3 \\ 7 \\ \vdots \\ (2N-1) \end{bmatrix}$$

Applications: The above results have been used with numerical optimisation algorithms in Reference 4 to find the discrete distributions which provide maximum difference directivity or maximum normalised difference slope, analogous to the continuous distributions derived earlier by Hannan[6] and Kirkpatrick,[5] respectively. They have also been used[4] in the extension of the method of Einarsson[3] to the problem of simultaneous synthesis of sum and difference arrays subject to feed network complexity restrictions. Details of these applications will shortly be submitted for publication.

D. A. McNAMARA

Department Electronics & Computer Engineering
University of Pretoria
Pretoria 0002, South Africa

16th December 1986

References

1 CHENG, D. K.: 'Optimisation techniques for antenna arrays', *Proc. IEEE*, 1971, **59**, pp. 1664–1674
2 KURTH, R.: 'Optimisation of array performance subject to multiple power pattern constraints', *IEEE Trans.*, 1974, **AP-22**, pp. 103–105
3 EINARSSON, O.: 'Optimisation of planar arrays', *ibid.*, 1979, **AP-27**, pp. 86–92
4 MCNAMARA, D. A.: 'On the synthesis of optimum monopulse antenna array distributions'. Thesis submitted for the degree of PhD in engineering at the University of Cape Town, Rondebosch 7700, South Africa
5 KIRKPATRICK, G. M.: 'Aperture illuminations for radar angle of arrival measurements', *IRE Trans.*, 1953, **AE-9**, pp. 20–27
6 HANNAN, P. W.: 'Maximum gain in monopulse difference mode', *ibid.*, 1961, **AP-9**, pp. 314–331

MILLIMETRE-WAVE PERFORMANCE OF STATE-OF-THE-ART MESFET, MODFET AND PBT TRANSISTORS

Indexing terms: Microwave devices and components, Transistors

It has recently been shown that, in addition to parasitics, the dipole domain which forms in FET-type devices produces a complex conjugate pole-pair which leads to a 12 dB/octave gain roll-off in the millimetre-wave region. As a result the actual F_{max} of millimetre-wave transistors is considerably less than that determined from the commonly used extrapolation of microwave frequency gain measurements at 6 dB per octave roll-off. Here device models are used to compare the millimetre-wave performance of state-of-the-art MESFET, MODFET and PBT transistors. A parametric study indicates that frequency performance is particularly sensitive to drain parasitics.

The gain and frequency performance of microwave and millimetre-wave transistors is described by Mason's gain U, the maximum stable gain G_{MS} and F_{max}, the frequency at which U and G_{MS} are unity.[1] While being difficult to measure, F_{max} is a particularly important figure of merit as it is the maximum frequency of oscillation and so indicates the boundary between an active and a passive device. Common practice has been to estimate F_{max} using extrapolation of microwave frequency gain measurements at -6 dB per octave, suggesting that reasonable gain can be obtained at frequencies well above 100 GHz. However, parasitics and domain capacitance can result in gain roll-off considerably higher than 6 dB/octave.[2,3] A more accurate approach to estimating F_{max} is to use a circuit model developed from physical insight as well as 2-port measurements. This is undertaken here as well as a parametric study to identify those parameters that currently limit frequency performance.

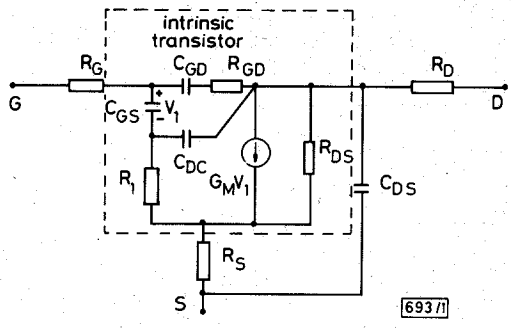

Fig. 1 *Circuit model of monolithically integrated transistor*
Lead inductances and packaging capacitances are not included so that the devices can be compared
$G_M = G_{M0}e^{-j\omega\tau}$, R_G, R_D and R_S are parasitic resistances, R_I is the resistance of the semiconductor channel, and C_{GD} and C_{DS} are essentially parasitic fringing capacitors. C_{DC} is the capacitance of the charge dipole domain that forms in the channel of FET-type devices.[9–11] With a PBT it is usual to use the bipolar transistor subscripts c, b and e instead of s, g and d

Circuit models with the topology of Fig. 1 have been developed for state-of-the-art MESFETs, a MODFET and a PBT yielding the element values of Table 1.[4–7] While C_{DC} of the MODFET was estimated, numerical studies[8] indicate that charge accumulation, and hence the domain capacitance C_{DC}, are comparable in MODFETs and MESFETs. The U responses of these transistors are shown in Fig. 2, and the extrapolated (from U at 1 GHz at a roll-off of 6 dB per octave) and calculated (using the model) values of F_{max} are given in Table 1. Extrapolated F_{max}s are up to 400 GHz, considerably greater than the calculated F_{max}s of around 100 GHz. The F_{max} of the intrinsic transistor, Fig. 1, is dominated by C_{DC}, Table 1, and is a fundamental limit of performance in the absence of parasitics. These results have significant implications for interpretations of F_{max} based on low-frequency gain

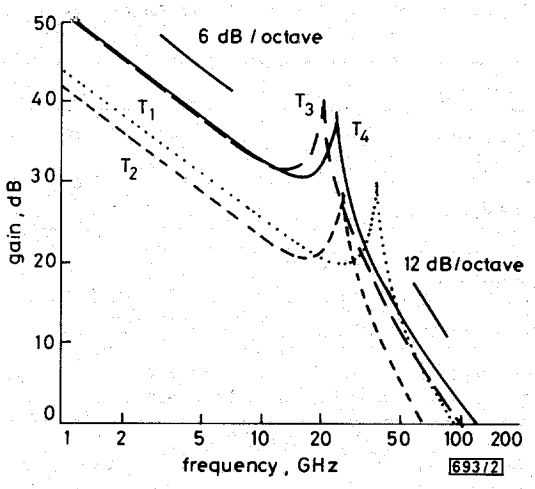

Fig. 2 *Calculated U of transistors*

measurements and extrapolation using the 6 dB per octave roll-off assumption. Such an extrapolation leads to erroneously high predictions of the millimetre-wave performance of microwave transistors. Positive feedback via C_{DC} increases low-frequency gain and induces a pole in U which, for millimetre-wave transistors, is typically below F_{max}. At frequencies below the induced pole C_{DC} can be left out of the model and its effect approximated by using a smaller value of C_{GS}.[2] Consequently it is difficult to determine C_{DC} from measurements taken at frequencies below that of the gain resonance.

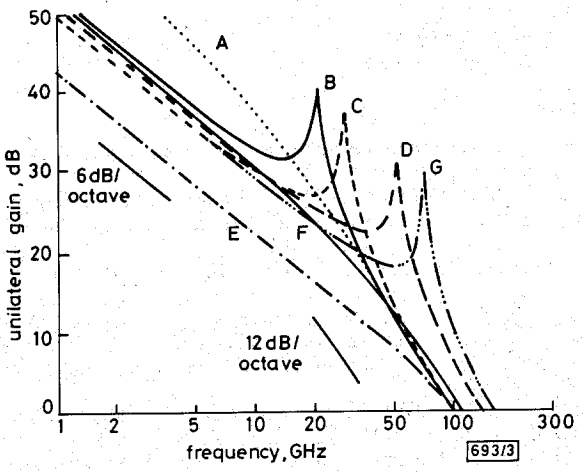

Fig. 3 *Calculated U of MESFET transistor* T_3

Curve B is the response of the actual transistor. The other curves are for the actual transistor but for curve A, $\tau = 0$ ($F_{max} = 96$ GHz); curve C, $C_{GD} = 0$ ($F_{max} = 97$ GHz); curve D, $C_{DS} = 0$ ($F_{max} = 140$ GHz); curve E, $C_{DC} = 0$ ($F_{max} = 97$ GHz); curve F, $R_S = 0$ ($F_{max} = 111$ GHz); curve G, $R_D = 0$ ($F_{max} = 163$ GHz)

Maki *et al.*'s MESFET has state-of-the-art performance and so a parametric study was undertaken of this transistor. The effect of an element being insignificant was modelled in the limit by eliminating the element from the model. The results are presented in Fig. 3, of which the major conclusion is that there is no simple relationship between low-frequency gain and F_{max}. For example, elimination of the domain capacitance, curve E, reduces the low-frequency gain of the transistor (by eliminating an internal positive feedback path) while having virtually no effect on F_{max}. Significant increases in F_{max} with little effect on low-frequency gain result from the elimination of a drain parasitic (C_{DS} or R_D).

Acknowledgments: This work was supported in part by the ITT GaAs Technology Center and the US Army under contract DAAG29-85-K-0185.

R. J. TREW
M. B. STEER

Department of Electrical & Computer Engineering
North Carolina State University
Raleigh, NC 27695-7911, USA

12th December 1986

References

1 TREW, R. J., STEER, M. B., and CHAMBERLAIN, D.: 'Parasitic effects upon the high-frequency performance of three-terminal devices'. 7–8 Oct. 1986, University of Duisburg, presented at 3rd GaAs simulation workshop

2 STEER, M. B., and TREW, R. J.: 'High frequency limits of millimetre-wave transistors', *IEEE Electron Device Lett.*, 1986, **EDL-7**, pp. 640–642

3 DAS, M. B., and SCHMIDT, P.: 'High-frequency limitations of abrupt-junction FET's', *IEEE Trans.*, 1973, **ED-20**, pp. 779–792

4 CHAO, P. C., PALMATEER, S. C., SMITH, P. M., MISHRA, U. K., DUH, K. H. G., and HWANG, J. C. M.: 'Millimeter-wave low-noise high electron mobility transistors', *IEEE Electron Device Lett.*, 1985, **EDL-6**, pp. 531–533

5 FENG, M., KANBER, H., EU, V. K., WATKINS, E., and HACKETT, L. R.: 'Ultrahigh frequency operation of ion-implanted GaAs metal-semiconductor field-effect transistors', *Appl. Phys. Lett.*, 1984, **44**, pp. 231–233

6 MAKI, D. W., SCHELLENBERG, J. M., YAMASAKI, H., and LIU, L. C. T.: 'A 69 GHz monolithic FET oscillator'. IEEE 1984 microwave and millimeter-wave monolithic circuits symposium digest of papers, 3–4 June 1984, pp. 62–66

Table 1 TRANSISTOR DATA

Device	T_1	T_2	T_3	T_4
Source	Chao[4]	Feng[5]	Maki[6]	Bozler[7]
Structure	0·25 × 150 μm	0·3 × 150 μm	0·25 × 60 μm	8 × 40 μm
Type	MODFET	MESFET	MESFET	PBT*
Parameter				
R_S, Ω	3·5	2·39	4·55	1·3
R_G, Ω	0·91	2·9	1·46	1·3
R_D, Ω	6·4	2·39†	6·7	0‡
R_I, Ω	4·62	0·94	2·69	0[3]
R_{DS}, Ω	208·3	258	556	432
R_{GD}, Ω	2·88	0	0	0
C_{GS}, pF	0·27	0·147	0·071	0·97
C_{GD}, pF	0·015	0·009	0·001	0·015
C_{DS}, pF	0·057	0·05†	0·025	0·036†
C_{DC}, pF	0·01†	0·03†	0·011	0‡
G_{M0}, mS	85·7	25·8	15·2	181
τ, ps	1	3†	1·25	4·2[4]
Full transistor model				
F_{max} extrapolated	197	132	400	430
F_{max} calculated	91	68	97	125
Intrinsic transistor with C_{DC}				
F_{max} extrapolated	282	395	450	—
F_{max} calculated	181	152	222	—
Intrinsic transistor without C_{DC}				
F_{max} extrapolated	169	236	250	—
F_{max} calculated	160	231	245	—

* Estimated based on parameters of similar devices
† Estimate not available
‡ Estimated from Reference 9

7 BOZLER, C. O., HOLLIS, M. A., NICHOLS, K. B., RABE, S., VERA, A., and CHEN, C. L.: '18·5 dB gain at 18 GHz with a permeable base transistor', *IEEE Electron Device Lett.*, 1985, **EDL-6**, pp. 456–458
8 TANG, J. Y.: 'Two-dimensional simulation of MODFET and GaAs gate heterojunction FET's', *IEEE Trans.*, 1985, **ED-32**, pp. 1817–1823
9 BOZLER, C. O., and ALLEY, G. D.: 'Fabrication and numerical simulation of the permeable base transistor', *ibid.*, 1980, **ED-27**, pp. 1128–1141
10 LIECHTI, C. A.: 'Microwave field-effect transistors—1976', *ibid.*, 1976, **MTT-24**, pp. 279–300
11 RAVAIOLI, U., and FERRY, D. K.: 'MODFET ensemble Monte Carlo model including the quasi-two-dimension electron gas', *ibid.*, 1986, **ED-33**, pp. 677–680

INTERFEROMETRIC MEASUREMENTS OF CHROMATIC AND POLARISATION MODE DISPERSION IN HIGHLY BIREFRINGENT SINGLE-MODE FIBRES

Indexing terms: Optical fibres, Polarisation, Optical measurement, Optical dispersion

Interferometric measurements on highly birefringent single-mode fibres have been performed. The group delay spectrum of each polarisation mode is independently measured over the whole 1·0–1·73 μm spectral range. The polarisation mode dispersion is obtained by direct subtraction of the group delay spectra.

Increasing interest in coherent optical communication systems and sensor applications in the past few years has led to a great effort in the development of polarisation-preserving single-mode fibres. Correspondingly, a similar effort must be made in the characterisation of the polarisation properties and related parameters of this new class of optical fibres. Several different polarisation-preserving fibres have been developed by enhancing the birefringence of the fibre to a degree high enough to decouple the two polarisation modes over long lengths of fibre. Therefore, among other properties, chromatic dispersion and polarisation mode dispersion (PMD) are of the greatest importance for coherent transmission systems or device applications.

Polarisation mode dispersion at a single wavelength had been measured in highly birefringent fibres by optical short pulse methods,[1] frequency domain[2,3] and interferometric techniques.[4] More recently, the interferometric technique using linear polarisers and a standard scanning Michelson interferometer was extended into the 0·9–1·5 μm range by using a white light source and Fourier transform spectroscopy.[5] In this letter we report simultaneous measurements of chromatic and polarisation mode dispersion of highly birefringent single-mode optical fibres using the interferometric method for group delay measurements in the 1·00–1·73 μm spectral range.

The experimental apparatus was a scanning all-fibre Michelson interferometer in which the group delay can be measured by the position of the fringe pattern with an accuracy of 1·6 fs. The ~1·85 m-long highly birefringent fibres were inserted into the test fibre arm and the group delay of each polarisation mode was compared to the group delay in the reference arm of the interferometer. Unpolarised light from a halogen lamp was scanned by a monochromator in the full 1·00–1·73 μm spectral range with an 8 nm spectral width.

Fig. 1 shows the direct measurement of the fringe contrast at $\lambda = 1{\cdot}30\,\mu m$ of a highly birefringent fibre. Owing to the different group velocities of each polarisation mode, the fringe pattern presents a double structure, each one corresponding to one polarisation mode. The relative intensity of the two peaks was found to be dependent on the orientation of the axes of the test fibre at the butt coupling to the interferometer, as well as on the residual birefringence of the fibre components of the interferometer. A comparison between the results for different butt coupling conditions showed, however, that the residual birefringence is negligibly small compared to that of the highly birefringent fibre.

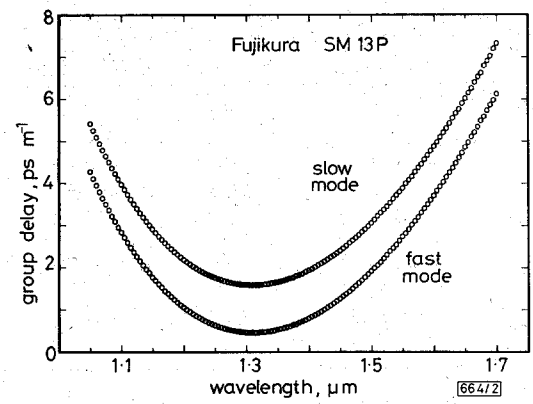

Fig. 2 *Grop delay spectra of two polarisation modes of a high-birefringence fibre*

Group delay measurements were carried on each 5 nm in the full spectral range of our apparatus for each polarisation mode. The corresponding results for the Fujikura SM13P fibre are displayed in Fig. 2. The group delay curves were fitted by a five-term Sellmeier expression and the chromatic dispersion of each polarisation mode obtained by simple differentiation of the fitted expression. The polarisation mode dispersion (PMD) at each wavelength was directly obtained by subtraction of the group delay data for each polarisation mode. Typical experimental results are shown in Fig. 3, together with the difference between the two five-term Sellmeier expressions fitting the group delays of each polarisation mode.

The computed results of dispersion measurements of different kinds of polarisation-preserving single-mode fibres are shown in Table 1, together with other measured parameters of the fibres used in the experiments. Fibres A and B present a strong index difference Δn and small core dimension. Despite the importance of the waveguide dispersion in the behaviour of these fibres, and the observed core ellipticity of fibres B and C, their PMD was found to be only slightly dependent on the wavelength. In this case, the wavelength-dependent geometrically induced birefringence is much smaller than the stress-induced birefringence,[6] so the resulting wavelength dependence is comparable to that of fibre A, which presents no core ellipticity.

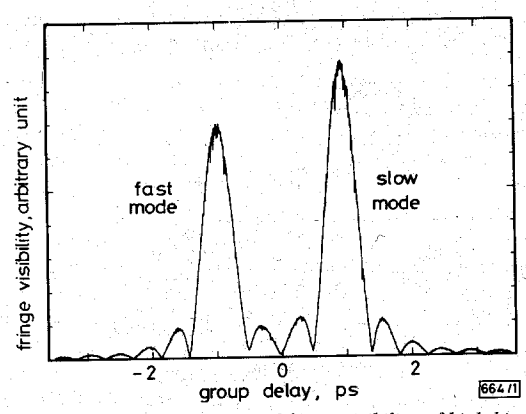

Fig. 1 *Direct measurement of fringe visibility of high-birefringence fibre at $\lambda = 1{\cdot}3\,\mu m$*

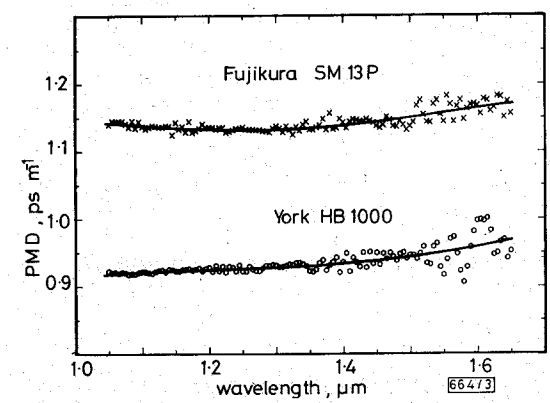

Fig. 3 *Polarisation mode dispersion of two different stress-induced high-birefringence fibres*